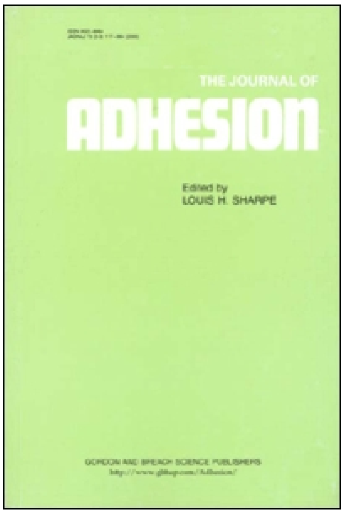

The Journal of Adhesion
Publication details, including instructions for authors and subscription information:
http://www.informaworld.com/smpp/title~content=t713453635

Low-rate Dynamic Contact Angles on Poly(methyl methacrylate/*n*-butyl methacrylate) and the Determination of Solid Surface Tensions

D. Y. Kwok[a]; C. N. C. Lam[a]; A. Li[a]; A. W. Neumann[a]
[a] Department of Mechanical and Industrial Engineering, University of Toronto, Toronto, Canada

To cite this Article Kwok, D. Y. , Lam, C. N. C. , Li, A. and Neumann, A. W.(1998) 'Low-rate Dynamic Contact Angles on Poly(methyl methacrylate/*n*-butyl methacrylate) and the Determination of Solid Surface Tensions', The Journal of Adhesion, 68: 3, 229 — 255

To link to this Article: DOI: 10.1080/00218469808029256
URL: http://dx.doi.org/10.1080/00218469808029256

J. Adhesion, 1998, Vol. 68, pp. 229-255
Reprints available directly from the publisher
Photocopying permitted by license only

Published by license under
the Gordon and Breach Science
Publishers imprint.
Printed in India.

Low-rate Dynamic Contact Angles on Poly(methyl methacrylate/*n*-butyl methacrylate) and the Determination of Solid Surface Tensions

D. Y. KWOK*, C. N. C. LAM, A. LI and A. W. NEUMANN†

Department of Mechanical and Industrial Engineering,
University of Toronto, 5 King's College Road, Toronto, Ontario, Canada M5S 3G8

(Received 6 October 1997; In final form 6 February 1998)

Low-rate dynamic contact angles of 12 liquids on a poly(methyl methacrylate/*n*-butyl methacrylate) P(MMA/*n*BMA) copolymer are measured by an automated axisymmetric drop shape analysis-profile (ADSA-P). It is found that 6 liquids yield non-constant contact angles, and/or dissolve the polymer on contact. From the experimental contact angles of the remaining 6 liquids, it is found that the liquid-vapour surface tension times the cosine of the contact angle changes smoothly with the liquid-vapour surface tension, *i.e.*, $\gamma_{lv}\cos\theta$ depends only on γ_{lv} for a given solid surface (or solid surface tension). This contact angle pattern is in harmony with those from other inert and non-inert (polar and non-polar) surfaces [34-42, 51-53]. The solid-vapour surface tension calculated from the equation-of-state approach for solid-liquid interfacial tensions [14] is found to be $34.4\,\mathrm{mJ/m^2}$, with a 95% confidence limit of $\pm 0.8\,\mathrm{mJ/m^2}$, from the experimental contact angles of the 6 liquids.

Keywords: Contact angle, dynamic; contact angle, equation of state; contact angle, drop shape; contact angle, complexity; surface tension, of solid; surface tension, from contact angle; surface tension, methacrylate copolymer

INTRODUCTION

Several independent approaches have been used to estimate solid surface tensions, including direct force measurements [1-9], contact

---

*This paper represents, in part, the Ph.D. thesis of D. Y. Kwok.
†Corresponding author.

angles [10–17], capillary penetration into columns of particle powder [18–21], sedimentation of particles [22–25], solidification fronts of particles [26, 27], gradient theory [28], and Lifshitz theory of van der Waals forces [28]. Among these methods, contact angle measurements are believed to be the simplest approach for surface energetics.

At the centre of contact angle research is Young's equation,

$$\gamma_{lv} \cos \theta_Y = \gamma_{sv} - \gamma_{sl} \tag{1}$$

which interrelates the Young contact angle with the interfacial tensions of the liquid–vapour γ_{lv}, solid–vapour γ_{sv} and solid–liquid γ_{sl} interfaces; θ_Y is the Young contact angle, *i.e.*, a contact angle which can be used in conjunction with Young's equation. While there are a number of thermodynamic equilibrium contact angles, θ_e, they are not necessarily equal to θ_Y [29–31].

Equation (1) implies a single, unique contact angle; in practice, however, contact angle phenomena are complicated [29–31]. For example, the contact angle made by an advancing liquid (θ_a) and that made by a receding liquid (θ_r) are not identical; nearly all solid surfaces exhibit contact angle hysteresis, H (the difference between θ_a and θ_r):

$$H = \theta_a - \theta_r \tag{2}$$

Contact angle hysteresis can be due to roughness heterogeneity of a solid surface. If roughness is the primary cause, then the measured contact angles are meaningless in terms of Young's equation. It is well known that on very rough surfaces, contact angles are larger than on chemically identical surfaces [21]; such angles do not reflect material properties of the surface; rather, they reflect morphological ones.

In general, the experimentally-observed apparent contact angle, θ, may or may not be equal to the Young contact angle, θ_Y [31]: (1) On ideal solid surfaces, there is no contact angle hysteresis and the experimentally observed contact angle is equal to θ_Y; (2) On smooth, but chemically heterogeneous solid surfaces, θ is not necessarily equal to the thermodynamic equilibrium angle. Nevertheless, the experimental advancing contact angle, θ_a, can be expected to be a good approximation of θ_Y. This has been illustrated using a model of heterogeneous (smooth) vertical strip surfaces [29, 31]. Therefore, care must be exercised to ensure that the experimental apparent contact angle, θ, is the advancing contact angle in order to be inserted into Young's equation; (3) On rough solid surfaces, no such equality between advancing contact angle and θ_Y exists. Thus, all contact angles on rough surfaces are meaningless in terms of Young's equation. While the receding angle on a heterogeneous and smooth surface can also be a Young angle, it is usually found to be non-reproducible often because of sorption of the liquid into the solid and swelling of the solid by the liquid [32].

Recently, we have shown [33–35] that measuring contact angles at very slow motion of the three-phase contact line allows direct observation of surface quality. In addition, when such procedures are interpreted by an automated axisymmetric drop shape analysis-profile (ADSA-P), complexities such as dissolution of the polymer by the liquid and slip/stick contact angles, which affect the contact interpretation in terms of surface energetics, can be identified [35–42].

In previous studies [40, 41], low-rate dynamic contact angles of various liquids were reported on two methacrylate homopolymers: poly(methyl methacrylate) PMMA and poly(*n*-butyl methacrylate) P*n*BMA. It was found that $\gamma_{lv}\cos\theta$ changes smoothly with γ_{lv}. Thus, one would expect that the results for a copolymer of the above methacrylate homopolymers should lie somewhere in between. Thus, it is the aim of this study to investigate this expectation for a poly(methyl methacrylate/*n*-butyl methacrylate) P(MMA/*n*BMA) copolymer. The P(MMA/*n*BMA)-coated surface is prepared by a solvent-casting technique; surface roughness is in the order of nanometers or less. These dynamic (advancing) contact angles are then employed for the interpretation in terms of solid surface tensions.

EXPERIMENTAL

Materials (Solid Surface and Liquids)

Poly(methyl methacrylate/*n*-butyl methacrylate) P(MMA/*n*BMA) copolymer was purchased from Polysciences (Warrington, P. A.; cat# 01922) as fine beads. A 2% P(MMA/*n*BMA)/chloroform solution was prepared using chloroform (Sigma-Aldrich, 99.9+% A.C.C. HPLC grade) as the solvent. Silicon wafers ⟨100⟩ (Silicon Sense, Nashua, N. H.; thickness: 525 ± 50 micron) were selected as the substrate for contact angle measurements. They were obtained as circular discs of about 10 cm diameter and were cut into rectangular shapes of about 2.5 cm × 5 cm. Each rectangular wafer surface was then soaked in chromic acid for at least 24 hrs., rinsed with doubly-distilled water, and dried under a heat lamp before polymer coating.

The P(MMA/*n*BMA)-coated surfaces were prepared by a solvent-casting technique: a few drops of the 2% P(MMA/*n*BMA)/chloroform solution were deposited on dried silicon wafers inside glass dishes overnight; the solution spread and a thin layer of the P(MMA/*n*BMA) formed on the wafer surface after the chloroform evaporated. This preparation produced good-quality coated surfaces, as manifested by light fringes due to refraction at these surfaces, suggesting that surface roughness is in the order of nanometers or less. The correctness of this reference has been confirmed broadly for such films, in Ref. [43] and other papers in preparation, by means of atomic force microscopy.

With respect to the low-rate dynamic contact angle measurements by ADSA-P, liquid was supplied to the sessile drop from below the wafer surfaces using a motorized syringe device [35, 36]. In order to facilitate such an experimental procedure, a hole of about 1 mm diameter was made, by using a diamond drill bit from Lunzer (NEW York, N.Y.; SMS-0.027), in the centre of each rectangular wafer surface before soaking in chromic acid. This strategy was pioneered by Oliver *et al.* [44, 45] to measure sessile drop contact angles because of its potential for avoiding drop vibrations and for measuring true advancing contact angles without disturbing the drop profile. In order to avoid leakage between a stainless steel needle (Chromatographic Specialities, Brockville, Ont; N723 needles pt. #3, H91023) and the hole (on the wafer surface), Teflon tape was wrapped around the end of the needle before insertion into the hole. In the literature, it is customary first to deposit a drop of liquid on a given solid surface using a syringe or a Teflon needle; the drop is then made to advance by supplying more liquid from above using a syringe or a needle in contact with the drop. Such experimental procedures cannot be used for ADSA-P since ADSA determines the contact angles and surface tensions based on a complete and undisturbed drop profile.

Twelve liquids were chosen in this study. Selection of these liquids was based on the following criteria: (1) they should include a wide

TABLE I Supplier, purity and surface tension of the liquids used

Liquid	*Supplier*	*%Purity*	*Density (g/cm^3)*	γ_{lv} *(mJ/m^2)*	*No. of drops*
dibenzylamine	aldrich	97	1.026	40.80 ± 0.06	9
dimethyl sulfoxide (DMSO)	sigma-aldrich	99.9 (HPLC)	1.101	42.68 ± 0.03	7
1-iodonaphthalene	aldrich	99	1.740	42.92 ± 0.03	10
1-bromonaphthalene	aldrich	98	1.489	44.31 ± 0.05	7
1,3-diiodopropane	aldrich	99	2.576	46.51 ± 0.13	10
3-pyridylcarbinol	aldrich	98	1.124	47.81 ± 0.03	10
1,1,2,2-tetrabromoethane	aldrich	98	2.967	49.29 ± 0.05	10
diiodomethane	aldrich	99	3.325	49.98 ± 0.02	10
2,2′-thiodiethanol	aldrich	99+	1.221	53.77 ± 0.03	10
formamide	aldrich	99.5+	1.134	59.08 ± 0.04	10
glycerol	baker analyzed	99.8	1.258	65.02 ± 0.04	8
water	LAST*	doubly distilled	0.977	72.70 ± 0.09	10

* Laboratory of applied surface thermodynamics.

range of intermolecular forces; (2) they should be non-toxic; and (3) the liquid surface tension should be higher than the anticipated solid surface tension [10, 14, 21]. They are listed in Table I, together with the physical properties and surface tensions (measured at 23.0 ± 0.5°C).

Methods and Procedures

ADSA-P is a technique to determine liquid–fluid interfacial tensions and contact angles from the shape of axisymmetric menisci, *i.e.*, from sessile as well as pendant drops [46]. Assuming that the experimental drop is Laplacian and axisymmetric, ADSA-P finds a theoretical profile that best matches the drop profile extracted from an image of a real drop, from which the surface tension, contact angle, drop volume, surface area and three-phase contact radius can be computed. The strategy employed is to fit the shape of an experimental drop to a theoretical drop profile according to the Laplace equation of capillarity, using surface/interfacial tension as an adjustable parameter. The best fit identifies the correct surface/interfacial tension from which the contact angle can be determined by a numerical integration of the Laplace equation. Details of the methodology and experimental set-up can be found elsewhere [35, 36, 46–48].

Sessile drop experiments were performed by ADSA-P to determine contact angles. The temperature and relative humidity were maintained, respectively, at 23.0 ± 0.5°C and at about 40%. It has been found that, since ADSA assumes as axisymmetric drop shape, the values of liquid surface tensions measured from sessile drops are very sensitive to even a very small amount of surface imperfection, such as roughness and heterogeneity, while contact angles are less sensitive. Therefore, the liquid surface tensions used in this study were independently measured by applying ADSA-P to a pendant drop, since the axisymmetry of the drop is enforced by using a circular capillary. Results of the liquid surface tension are given in Table I.

In this study, 6 dynamic contact angle measurements at velocities of the three-phase contact line in the range from 0.1 to 1.1 mm/min were performed for each liquid. The choice of this velocity range was based on previous studies [33–36] which showed that low-rate dynamic contact angles at these velocities are essentially identical to the static contact angles, for these relatively smooth surfaces.

In actual experiments, an initial liquid drop of about 0.3 cm radius was carefully deposited, covering the hole on the surface. This is to ensure that the drop will increase axisymmetrically in the centre of the image field when liquid is supplied from the bottom of the surface and will not hinge on the lip of the hole. The motor in the motorized syringe mechanism was then set to a specific speed, by adjusting the voltage from a voltage controller. Such a syringe mechanism pushes the syringe plunger, leading to an increase in drop volume and, hence, the three-phase contact radius. A sequence of pictures of the growing drop was then recorded by the computer typically at a rate of 1 picture every 2–5 seconds, until the three-phase contact radius was about 0.5 cm or larger. For each low-rate dynamic contact angle experiment, at least 50 and up to 200 images were normally taken. Since ADSA-P determines the contact angle and the three-phase contact radius simultaneously for each image, the advancing dynamic contact angles as a function of the three-phase contact radius (*i.e.*, location on the surface) can be obtained. The actual rate of advancing can be determined by linear regression, by plotting the three-phase contact radius over time. For each liquid, different rates of advancing were studied, by adjusting the speed of the pumping mechanism.

It should be noted that measuring contact angles as a function of the three-phase contact radius has an additional advantage: the quality of the surface is observed indirectly in the measured contact angles. If a solid is not very smooth, irregular and inconsistent angle values will be seen as a function of the three-phase contact radius. When the measured contact angles are essentially constant at different surface locations, the mean contact angle for a specific rate of advancing can be obtained by averaging the contact angles, after the three-phase contact radius reaches 0.4 to 0.5 cm (see later). The purpose of choosing these relatively large drops is to avoid any line tension effects on the measured contact angles [49, 50].

RESULTS AND DISCUSSION

Of the 12 liquids used, it was found that only 6 liquids yielded usable contact angles. They are water, glycerol, formamide, 2,2′-thiodiethanol, 3-pyridylcarbinol, and 1-iodonaphthalene. The remaining 6 liquids either dissolved the polymer on contact or yielded non-constant contact angles during the course of the experiments.

Figure 1(a)–(f) show, respectively, typical experimental results of water, glycerol, formamide, 2,2′-thiodiethanol, 3-pyridylcarbinol, and 1-iodonaphthalene: all contact angles are essentially constant, as the drop volume, V, increases and, hence, the three-phase contact radius, R. Increasing the drop volume in this manner ensures the measured θ to be an advancing contact angle. In all these cases, the measured contact angles are essentially constant as R increases. This indicates good quality of the surfaces used. It turns out that averaging the measured contact angles after R reaches 0.4 cm is convenient, since the drop is guaranteed to be in the advancing mode and that line tension effects are negligible. While this may seem to be an arbitrary value, it turns out that there is virtually no dependence on the choice of the starting point.

In Figures 1(a) and (b), the contact angles of water and glycerol increase initially at essentially constant R. This is due to the fact that even carefully putting an initial drop from above the surface can result in contact angles somewhere between advancing and receding. Thus, after reaching the proper advancing angles, the drop front starts to

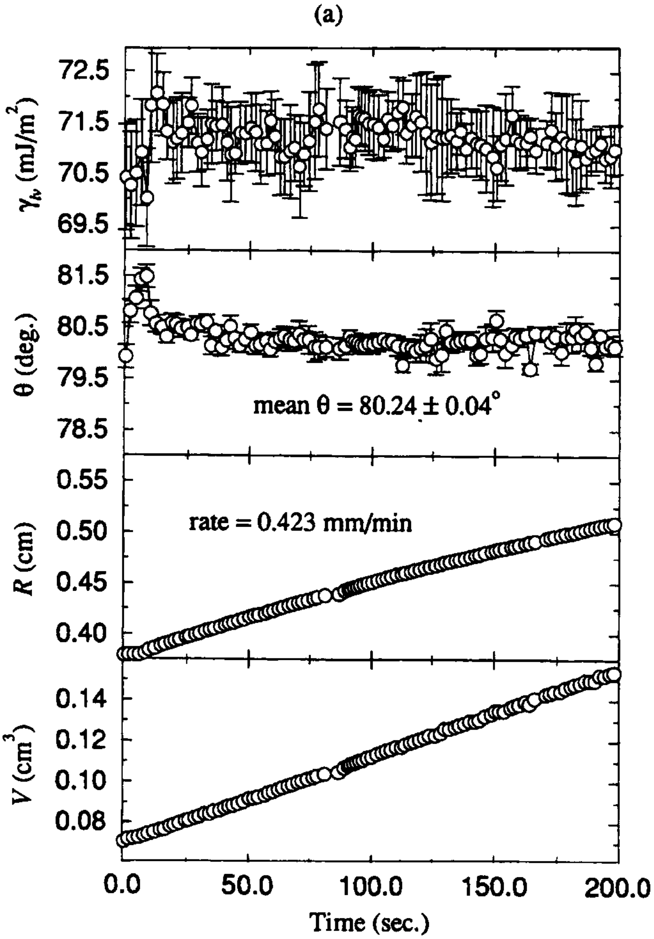

FIGURE 1 Low-rate dynamic contact angles on a P(MMA/*n*BMA)-coated wafer surface for (a) water; (b) glycerol; (c) formamide; (d) 2,2′-thiodiethanol; (e) 3-pyridylcarbinol; and (f) 1-iodonaphthalene.

advance with essentially constant θ. It should be noted that the liquid–vapour surface tension values calculated by ADSA-P sessile drop are fairly constant, but not as reliable as those from pendant drop, as explained above. The accuracy relies very much on the axisymmetry of the drop profile.

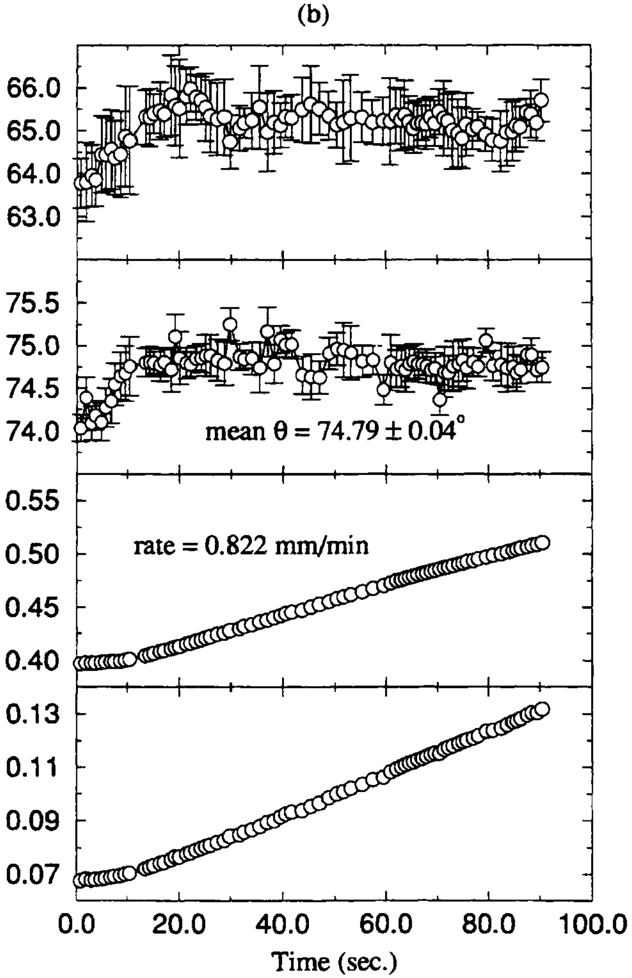

FIGURE 1 (Continued).

Two liquids, 1,1,2,2-tetrabromoethane and dibenzylamine, were found to dissolve the P(MMA/*n*BMA)-coated wafer on contact, resulting in irregular and flat drops. The remaining 4 liquids all show very complex contact angle behaviour, as given in Figures 2(a)–(d). Figure 2(a) shows the contact angle results of diiodomethane. It can be seen that initially the apparent drop volume, as perceived by ADSA-P,

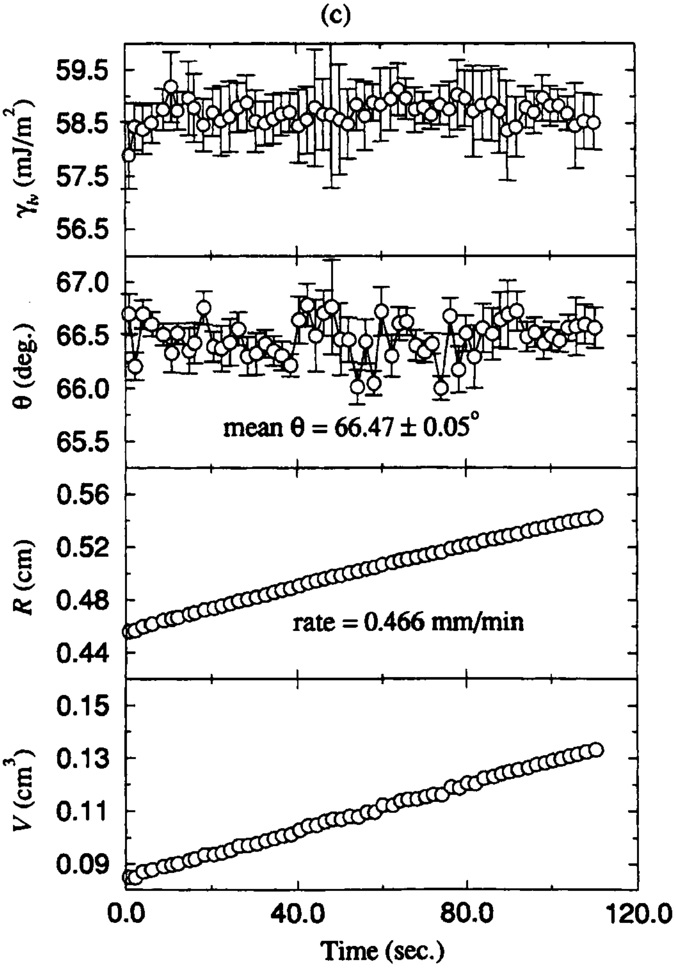

FIGURE 1 (Continued).

increases linearly, and θ increases from 50° to 80° at essentially constant R. Suddenly, the drop front jumps to a new location as more liquid is supplied into the sessile drop. The resulting θ decreases sharply from 80° to 45°. As more liquid is supplied into the sessile drop, the contact angle increases again. Such slip/stick behaviour could be due to non-inertness of the surface. Phenomenologically, an energy barrier for the drop front exists, resulting in sticking, which

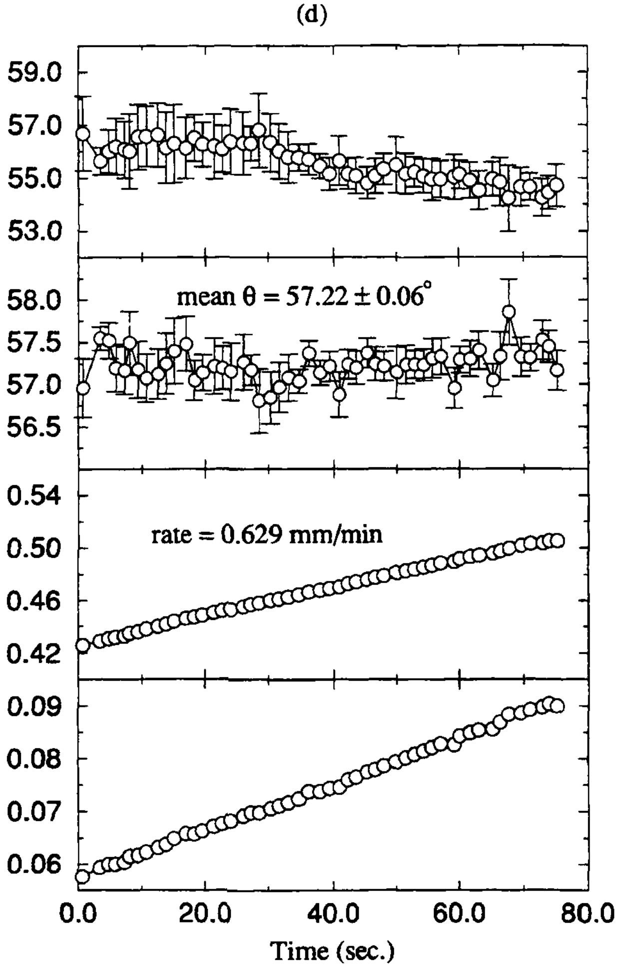

FIGURE 1 (Continued).

causes θ to increase at constant R. However, as more liquid is supplied into the sessile drop, the drop front possesses enough energy to overcome the energy barrier, resulting in slipping, which causes θ to decrease suddenly. It should be noted that as the drop front jumps from one location to the next, it is unlikely that the drop is, or will remain, axisymmetric. Such a non-axisymmetric drop will obviously not meet the basic assumption underlying ADSA-P, causing possible

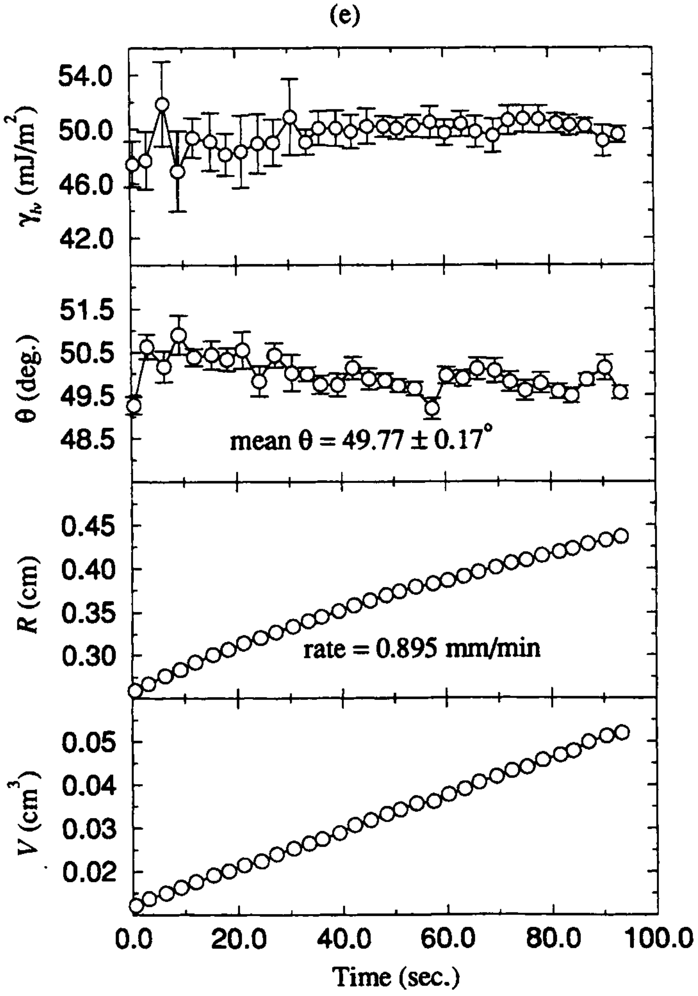

FIGURE 1 (Continued).

errors, *e.g.*, in the apparent surface tension and drop voulme. This can be seen from the discontinuity of the apparent surface tension and drop volume with time as the drop front sticks and slips. Obviously, the observed angles in Figure 2(a) cannot all be the Young contact angles; since γ_{lv}, γ_{sv} (and γ_{sl}) are constants, θ ought to be a constant because of Young's equation. In addition, it is difficult to decide

(f)

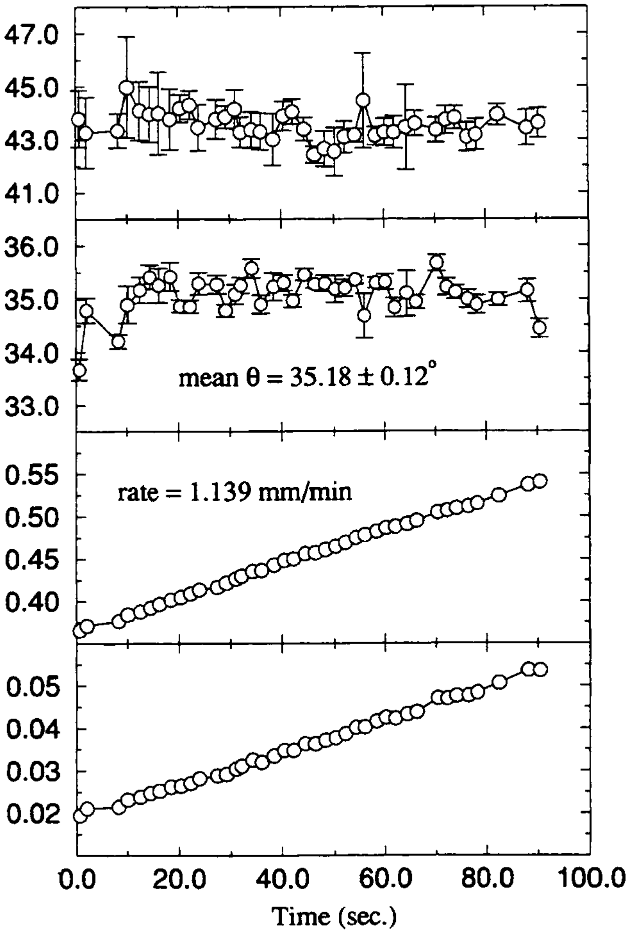

FIGURE 1 (Continued).

unambiguously at this moment whether or not Young's equation is applicable at all because of lack of understanding of the slip/stick mechanism. Therefore, these contact angles should not be used for the interpretation in terms of surface energetics. Although of no direct consequence to the present study, we point out that, recently, a theory has been proposed [50] which provides a simple explanation for the slip/stick motion of the three-phase contact line. This approach

(a)

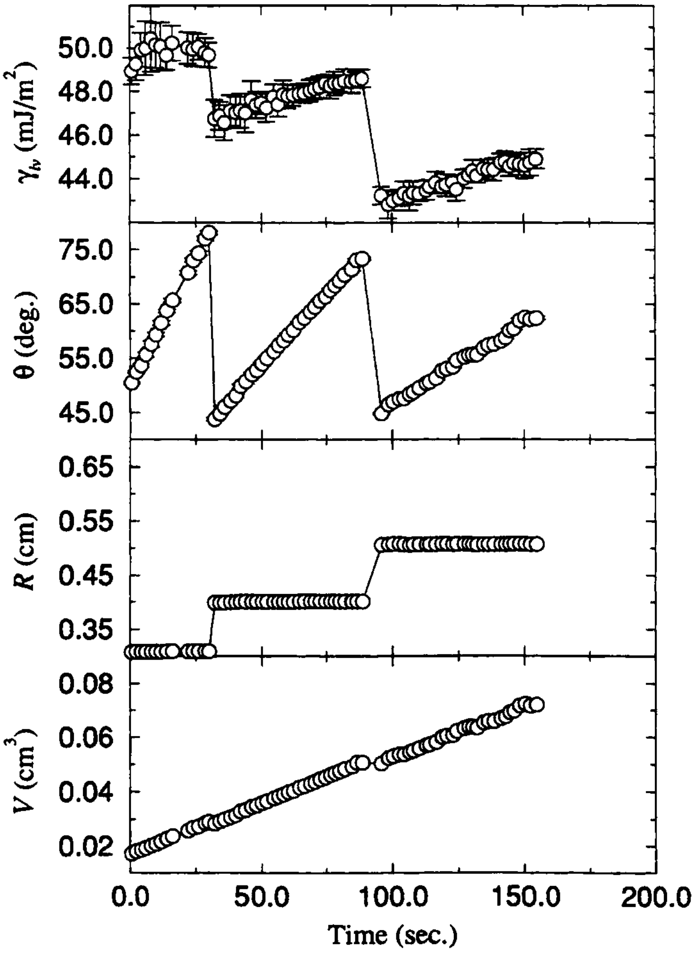

FIGURE 2 Low-rate dynamic contact angles on a P(MMA/*n*BMA)-coated wafer surface for (a) diiodomethane; (b) 1,3-diiodopropane; (c) 1-bromonaphthalene; and (d) dimethyl sulfoxide (DMSO). These angles cannot be used for the interpretation in terms of surface energetics, see text.

accounts for the effects of evaporation on the contact angles at constant three-phase contact radius.

A different contact angle pattern can be seen in Figure 2(c) for 1-bromonaphthalene, where γ_{lv} and θ decrease from that of the pure

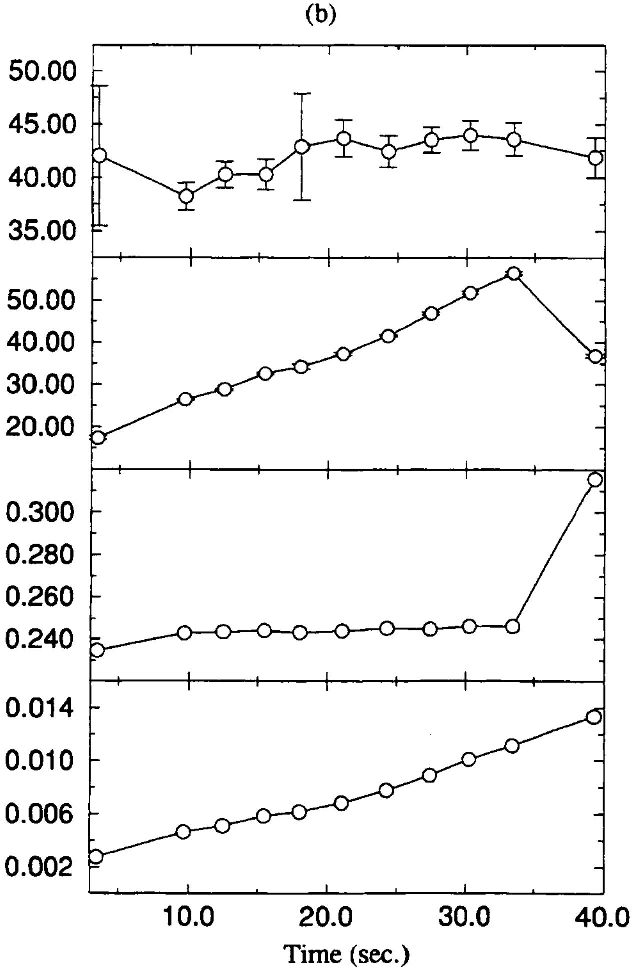

FIGURE 2 (Continued).

liquid and with time. It should be noted that yet another contact angle pattern is given in Figure 2(d) for dimethyl sulfoxide (DMSO): θ increases at the beginning and decreases as the experiment proceeded. In both cases, the copolymer in the contact area between the liquids and P(MMA/*n*BMA) was observed to be partly removed after the experiments. This suggests that dissolution of P(MMA/*n*BMA) by the liquids occurs. Since the observations force us to discard the

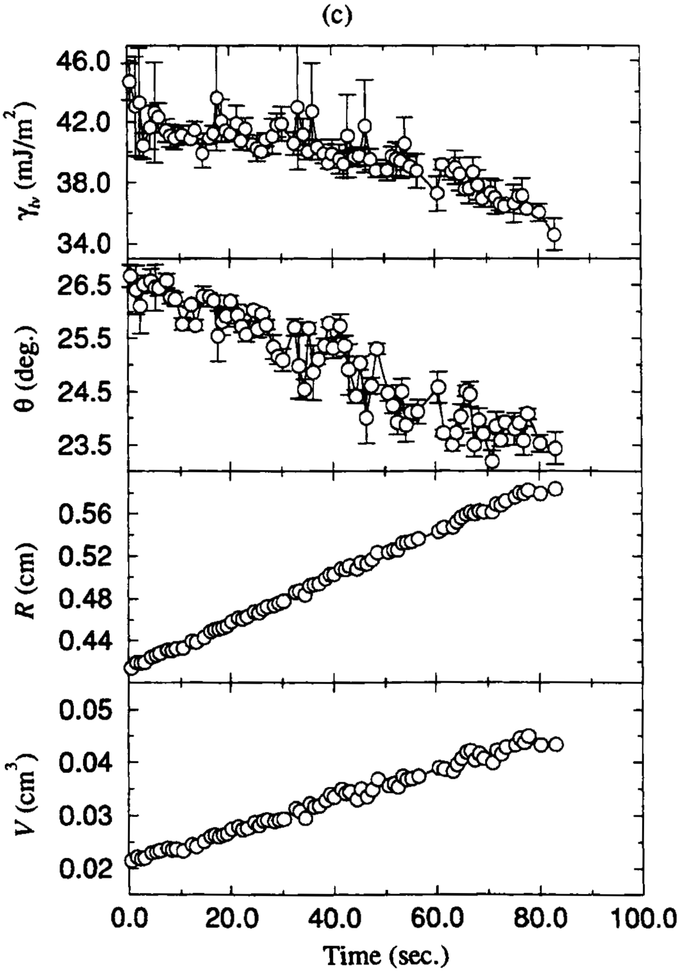

FIGURE 2 (Continued).

measurement it is not necessary to verify our stipulation of dissolution of the copolymer by the liquid. If desired, such a verification can readily be performed, *e.g.*, by measuring the refractive index. Even if polymer dissolution would not be the cause of the observed pattern, the measurement would have to be discarded. Obviously, these angles should be disregarded for the following reasons: (1) γ_{lv} is different

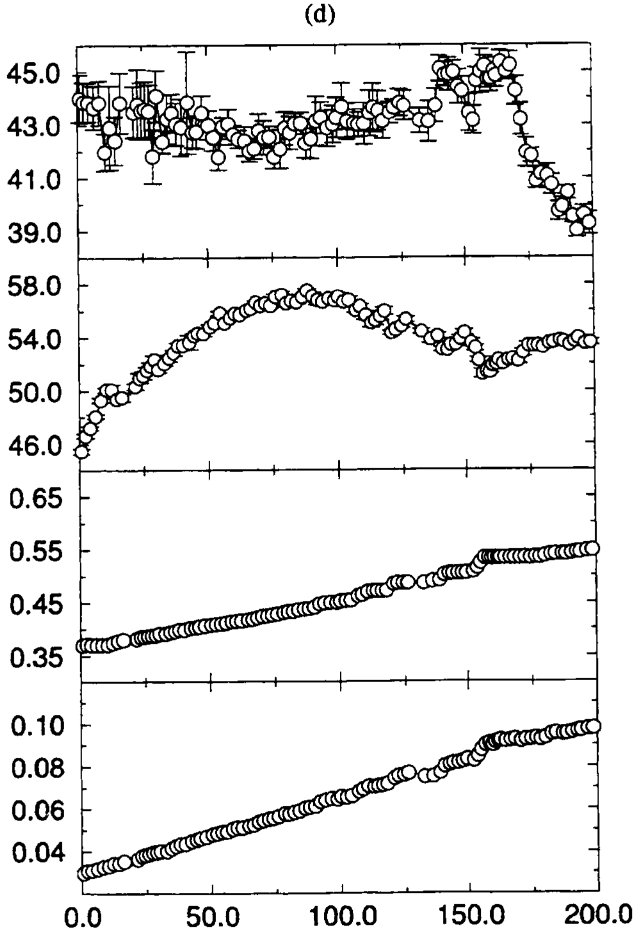

FIGURE 2 (Continued).

from that of the pure liquids; (2) we are unsure whether or not γ_{sl} and γ_{sv} remain constant and whether Young's equation is applicable.

The reproducibility of all solid–liquid systems is very good. They are summarized in Table II for the 6 liquids with usable contact angles, at different rates of advancing and each on a newly-prepared surface. It should be noted that a total of more than 70 freshly-prepared

P*n*BMA-coated wafers were prepared and used; more than 5,000 images were acquired and analyzed by ADSA-P. In the specific case of water in Table II, a final value of $\theta = 81.33° \pm 0.80°$ was obtained, by averaging the contact angles from different rates of advancing (for different experiments). The 95% confidence limits calculated in this manner (in Tab. II) include all possible errors, due to experimental technique, solid surface preparation, *etc.* A summary of the contact angle complexities is given in Table III, together with the meaningful results from Table II.

Disregarding the inconclusive contact angle data in Figure 2, we show in Figure 3 the contact angle results from Table II, by plotting $\gamma_{lv} \cos\theta$ *vs.* γ_{lv}, together with the error limits calculated from the

TABLE II Summary of the advancing contact angles (deg.) at different rates (mm/min.) of motion of the three-phase contact line for liquids which yielded constant contact angles on a poly(methyl methacrylate/*n*-butyl methacrylate) P(MMA/*n*BMA)-coated silicon wafer

Water		*Glycerol*		*Formamide*	
rate	*θ*	*rate*	*θ*	*rate*	*θ*
0.265	82.67 ± 0.07	0.321	75.65 ± 0.06	0.424	65.70 ± 0.07
0.300	82.86 ± 0.07	0.358	74.53 ± 0.05	0.425	66.58 ± 0.04
0.333	82.89 ± 0.13	0.359	75.04 ± 0.07	0.441	66.62 ± 0.06
0.348	80.35 ± 0.05	0.409	74.67 ± 0.07	0.456	66.64 ± 0.04
0.423	80.24 ± 0.04	0.456	73.46 ± 0.07	0.466	66.47 ± 0.05
0.562	80.29 ± 0.04	0.682	74.48 ± 0.04	0.809	66.07 ± 0.12
0.568	80.94 ± 0.05	0.702	74.52 ± 0.09	0.812	67.12 ± 0.13
0.578	81.42 ± 0.07	0.822	74.79 ± 0.04	0.874	65.71 ± 0.15
0.603	81.53 ± 0.24	–	–	0.964	66.02 ± 0.14
0.693	80.06 ± 0.08	–	–	–	–
	81.33 ± 0.80*		74.72 ± 0.59*		66.33 ± 0.37*
2,2′-*thiodiethanol*		3-*pyridylcarbinol*		1-*iodonaphthalene*	
rate	*θ*	*rate*	*θ*	*rate*	*θ*
0.313	57.51 ± 0.18	0.516	48.91 ± 0.09	0.201	36.01 ± 0.35
0.331	58.46 ± 0.07	0.576	48.98 ± 0.08	0.382	35.28 ± 0.23
0.491	58.48 ± 0.05	0.850	49.57 ± 0.14	0.552	35.92 ± 0.14
0.505	57.31 ± 0.04	0.866	48.88 ± 0.07	0.601	35.04 ± 0.19
0.562	57.84 ± 0.05	0.895	49.77 ± 0.17	0.870	36.28 ± 0.10
0.625	58.36 ± 0.10	–	–	0.904	36.48 ± 0.09
0.629	57.22 ± 0.06	–	–	0.920	35.37 ± 0.19
0.896	57.56 ± 0.12	–	–	0.929	35.24 ± 0.16
–	–	–	–	0.930	35.92 ± 0.40
–	–	–	–	1.139	35.18 ± 0.12
	57.84 ± 0.44*		49.22 ± 0.52*		35.67 ± 0.36*

* mean θ value with the 95% confidence limits.

TABLE III Summary of contact angle results for a poly(methyl methacrylate/*n*-butyl methacrylate) P(MMA/*n*BMA)-coated silicon wafer surface

Liquids	γ_{lv} (mJ/m^2)	θ (*deg.*)
dibenzylamine	40.80	dissolved the copolymer on contact
dimethyl sulfoxide (DMSO)	42.68	$\theta\uparrow\downarrow$ as $R\uparrow$ (46° → 56° → 51°)*
1-iodonaphthalene	42.92	35.67 ± 0.36
1-bromonaphthalene	44.31	$\theta\downarrow$ and $\gamma_{lv}\downarrow$ as $R\uparrow$ (27° → 23°)*
1,3-diiodopropane	46.51	slip/stick (15° → 55°)*
3-pyridylcarbinol	47.81	49.22 ± 0.52
1,1,2,2-tetrabromoethane	49.29	dissolved the copolymer on contact
diiodomethane	49.98	slip/stick (45° → 75°)
2,2'-thiodiethanol	53.77	57.84 ± 0.44
formamide	59.08	66.33 ± 0.37
glycerol	65.02	74.72 ± 0.59
water	72.70	81.33 ± 0.80

* Part of the copolymer was observed to be removed after the experiment.

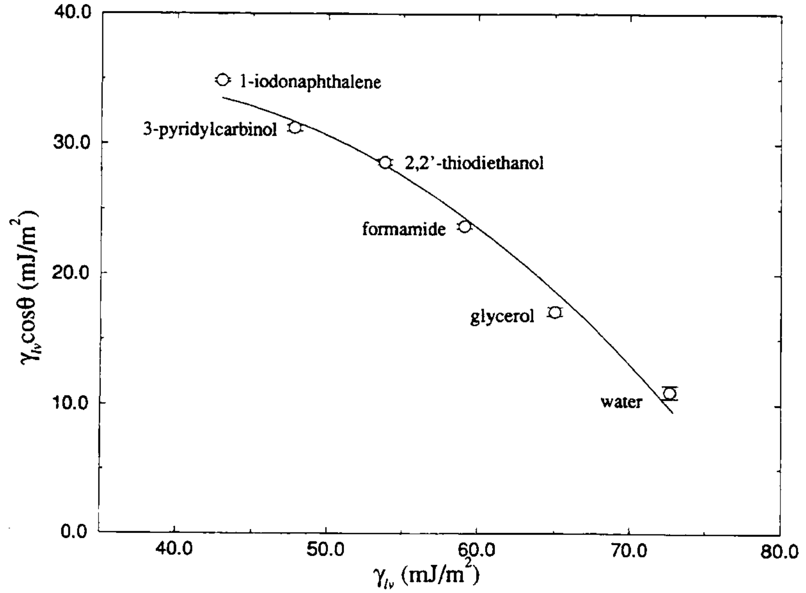

FIGURE 3 The values of $\gamma_{lv}\cos\theta$ *vs.* γ_{lv} for the P(MMA/*n*BMA)-coated wafer surface, for the data in Table II. Since the values of $\gamma_{lv}\cos\theta$ change smoothly with γ_{lv} at constant γ_{sv}, γ_{sl} can be expressed as a function of only γ_{lv} and γ_{sv} because of Young's equation.

contact angle errors. It can be seen that all liquids, independent of molecular properties, fall on a smooth curve, in agreement with the patterns obtained in previous studies [34–42, 52–54]: the values of γ_{lv} cos θ change smoothly with γ_{lv}, so that we again conclude that

$$\gamma_{lv}\cos\theta = F(\gamma_{lv}, \gamma_{sv}) \tag{3}$$

and hence, because of Young's equation

$$\gamma_{sl} = f(\gamma_{lv}, \gamma_{sv}) \tag{4}$$

Thus, the surface tension component approaches [11, 15–17] clash directly with these experimental results: the surface tension component approaches [11, 15–17] stipulate that γ_{sl} depends not only on γ_{lv} and γ_{sv}, but also on the specific intermolecular forces of the liquids and solids. But the above experimental results allow one to search for a relation in the form of Eq. (4).

On phenomenological grounds, an equation-of-state approach for solid–liquid interfacial tensions has been formulated [14]:

$$\gamma_{sl} = \gamma_{lv} + \gamma_{sv} - 2\sqrt{\gamma_{lv}\gamma_{sv}}\; e^{-\beta(\gamma_{lv}-\gamma_{sv})^2} \tag{5}$$

where β is a constant which was found to be 0.0001247 $(\text{m}^2/\text{mJ})^2$. Combining this equation with Young's equation yields

$$\cos\theta_Y = -1 + 2\sqrt{\frac{\gamma_{sv}}{\gamma_{lv}}}\; e^{-\beta(\gamma_{lv}-\gamma_{sv})^2} \tag{6}$$

Thus, the solid surface tensions can be determined from experimental (Young) contact angles and liquid surface tensions.

The applicability of any approach having the form of Eq. (4) can be tested using the criteria of the constancy of the calculated γ_{sv} values. Relations of the form of Eq. (4) have been in the literature for a long time. Two examples are Antonow's rule [55]

$$\gamma_{sl} = |\gamma_{lv} - \gamma_{sv}| \tag{7}$$

and Berthelot's geometric mean relationship [55]

$$\gamma_{sl} = \gamma_{lv} + \gamma_{sv} - 2\sqrt{\gamma_{lv}\gamma_{sv}} \tag{8}$$

Combining these or similar relationships with Young's equation yields a relation of the form of Eq. (3), from which γ_{sv} can be calculated. We show in Table IV the γ_{sv} values calculated from Antonow's rule [55], Berthelot' rule [56], and the equation-of-state approach for solid–liquid interfacial tension [14], *i.e.*, Eq. (6), which can be understood as a modified Berthelot rule [57]. It can be seen that the values of γ_{sv} calculated from Antonow's rule increase as γ_{lv} increases; the γ_{sv} values calculated from Berthelot's rule decrease γ_{lv} increases. Only the γ_{sv} values from the equation-of-state approach for solid–liquid interfacial tensions are quite constant, essentially independent of the liquids used: the γ_{sv} value of P(MMA/*n*BMA) was found to be 34.40 mJ/m^2 with a 95% confidence limit of ± 0.83% mJ/m^2.

It should be noted that the constant β value of 0.0001247 (m^2/mJ)^2 used in the above calculations had been obtained only from contact angle data on three well-prepared solid surfaces [51]: FC-721-coated mica, heat-pressed Teflon (FEP), and poly(ethylene terephthalate) (PET). Alternatively, the γ_{sv} value of P(MMA/*n*BMA) can be determined a two-variable least-square analysis [14], by assuming γ_{sv} and β in Eq. (6) to be constant. In this procedure, the computer will search for that pair of γ_{sv} and β values which provides the best fit of Eq. (6) to the six pairs of experimental (θ_Y, γ_{lv}) data points. This leads to a β value of 0.0001362 (m^2/mJ)^2 and a γ_{sv} value of 34.66 mJ/m^2. It is evident that there is good agreement between the γ_{sv} values (34.40 ± 0.83 mJ/m^2 and 34.66 mJ/m^2) determined from the two strategies. However, it might be argued that the two β values are

TABLE IV The solid–vapour surface tension values, γ_{sv}, of a poly(methyl methacrylate/*n*-butyl methacrylate) P(MMA/*n*BMA)-coated silicon wafer surface calculated from Antonow's rule [55], Berthelot's [56] and the equation-of-state approach for solid–liquid interfacial tensions [14]

Liquids	γ_{lv} *(mJ/m^2)*	θ *(deg.)*	γ_{sv} *(mJ/m^2)*		
			Antonow's rule	*Berthelot's rule*	*Equation-of-state*
1-iodonaphthalene	42.92	35.67 ± 0.36	38.89	35.25	35.71
3-pyridylcarbinol	47.81	49.22 ± 0.52	39.52	32.67	34.21
2,2'-thiodiethanol	53.77	57.84 ± 0.44	41.20	31.56	34.59
formamide	59.08	66.33 ± 0.37	41.40	29.01	33.96
glycerol	65.02	74.72 ± 0.59	41.08	25.95	33.34
water	72.70	81.33 ± 0.80	41.83	24.07	34.58

different. To show that such a difference is of little consequence with respect to the determination of γ_{sv}, we determine the γ_{sv} values of a hypothetical system having $\gamma_{lv} = 50\,\mathrm{mJ/m^2}$ and $\theta = 50°$ for the above β values. It turns out that there are virtually no differences in the calculated γ_{sv} values: $\gamma_{sv} = 35.54\,\mathrm{mJ/m^2}$ when $\beta = 0.0001247\,(\mathrm{m^2/mJ})^2$ and $\gamma_{sv} = 35.67\,\mathrm{mJ/m^2}$ when $\beta = 0.0001362\,(\mathrm{m^2/mJ})^2$.

Obviously, because of Eq. (6), the contact angles for any liquid can be predicted from the γ_{sv} value obtained from a single point of (θ_Y, γ_{lv}). This is illustrated in Table V; from the experimental values of γ_{lv} and θ for 2,2′-thiodiethanol Eq. (6) yields $\gamma_{sv} = 34.59\,\mathrm{mJ/m^2}$. With this value of γ_{sv}, the contact angles for the remaining 5 liquids are calculated from Eq. (6) and listed in Table V. It is apparent that the predicted contact angles agree with the experimentally-observed ones to within approximately ±2°, *i.e.*, the accuracy/reproducibility normally associated with contact angle measurements. It is apparent that surface tensions determine the contact angles completely; the specific intermolecular forces which give rise to the surface tensions do not affect the contact angles directly. The difference between the predicted and measured angles are indeed very small and could not even be detected if a conventional contact angle technique were used.

The above results indeed reconfirm the validity of the equation-of-state approach [14] to determine solid surface tensions from contact angles.

The fact that $\gamma_{lv}\cos\theta$ changes smoothly with γ_{lv} for the (PMMA/*n*BMA) copolymer should be confronted with the results obtained in previous studies [40, 41] for the two methacrylate homopolymers: poly(methyl methacrylate) PMMA and poly(*n*-butyl methacrylate) P*n*BMA. We show in Figure 4 these contact angle results, together with the results for the P(MMA/*n*BMA) copolymer. Again, $\gamma_{lv}\cos\theta$

TABLE V The predicted contact angles for the liquids based solely on the contact angle and surface tension of 2,2′-thiodiethanol ($\gamma_{sv} = 34.59\,\mathrm{mJ/m^2}$) using Eq. (6)

Liquids	γ_{lv} (mJ/m^2)	*Measured* θ (*deg.*)	*Predicted* θ (*deg.*)
1-iodonaphthalene	42.92	35.67 ± 0.36	38.74
3-pyridylcarbinol	47.81	49.22 ± 0.52	48.36
formamide	59.08	66.33 ± 0.37	65.16
glycerol	65.02	74.72 ± 0.59	72.56
water	72.70	81.33 ± 0.80	81.31

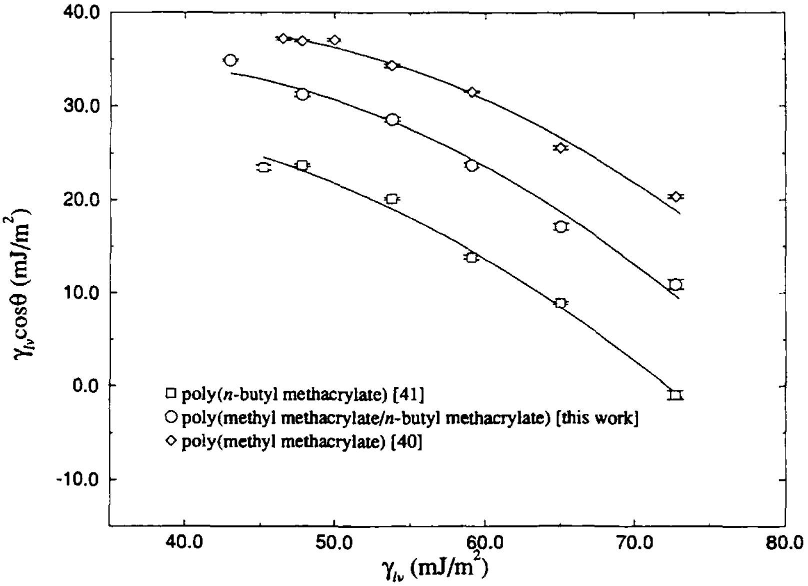

FIGURE 4 The values of $\gamma_{lv}\cos\theta$ *vs.* γ_{lv} for the P*n*BMA-, P(MMA/*n*BMA)-, and PMMA-coated wafer surface. Again, $\gamma_{lv}\cos\theta$ changes smoothly with γ_{lv} at constant γ_{sv}.

changes smoothly and systematically with γ_{lv} and γ_{sv}: varying the length of the side chain shifts the curves in a regular and expected manner. The γ_{sv} values of P*n*BMA [41] and PMMA [40] are found from the equation-of-state approach to be, respectively, $28.8 \pm 0.5\,\mathrm{mJ/m^2}$ and $38.5 \pm 0.5\,\mathrm{mJ/m^2}$, so that the value for P(MMA/*n*BMA) is intermediate, as expected.

As Figure 4 stands, there might be two possible concerns: the first one is whether such data could simply be represented by straight lines; the next one is whether the curves are indeed smooth.

With respect to the first point, statistical tools provide a definitive answer. We have performed a least-square analysis to fit these experimental contact angle data separately with linear and, for simplicity, quadratic equations. The results are given in Table VI. To illustrate the generality of such patterns, contact angle data on a FC-722-coated mica surface [35] are also used. It can be seen in Table VI that, in all cases, the regression coefficients for quadratic equations are better than those of the linear equations and that curvature is

TABLE VI A summary of the regression results using linear and quadratic equations, see text

Surfaces	R^2 *(regression coefficient)*	
	Linear equation	*Quadratic equation*
poly(*n*-butyl methacrylate) P*n*BMA [41]	0.968	0.994
poly(methyl methacrylate/*n*-butyl methacrylate) P(MMA/*n*BMA) [this work]	0.985	0.994
poly(methyl methacrylate) PMMA [40]	0.976	0.990
FC-722-coated mica [35]	0.963	0.997

indeed present in the plots of these data, *i.e.*, even a simple quadratic equation represents the data better than a linear equation; use of Eq. (6) would be expected to give a better fit yet.

With respect to the second point, it does not appear to us that there is any systematic change in the contact angles (in Fig. 4): For example, in the case of 3-pyridylcarbinol, with γ_{lv} about 48.0 mJ/m^2, the data point on the PMMA curve appears to be slightly higher, while the point on the P(MMA/*n*BMA) is slightly lower and the one for P*n*BMA slightly higher again. There is no evidence for any systematic variation, for this and other liquids. Clearly, if there were a deviation due to specific intermolecular forces, one would, at the most, expect a monotonous change of the deviation when going from PMMA to P(MMA/*n*-BMA) to P*n*BMA. To help out matters in perspective, it has to be realized that the curves in Figure 4 would have to be considered smooth if conventional goniometric techniques with ± 2° contact angle accuracy were used. Further, the fact that an equilibrium spreading pressure of as low as 1 mJ/m^2 would easily contribute to such a variation should not be overlooked; even very minor swelling of the polymer or creeping of the liquid could easily introduce a slight deviation of the polymer from such curves. Therefore, only after considering such effects would the need arise for explanations in terms of direct effects of intermolecular forces [58].

CONCLUSIONS

(1) The values of $\gamma_{lv}\cos\theta$ change smoothly with γ_{lv}, in excellent agreement with those from other polar and non-polar solid surfaces [34–42, 51–53].

(2) The γ_{sv} values of poly(methyl methacrylate/*n*-butyl methacrylate) P(MMA/*n*BMA) copolymer calculated from the equation-of-state approach [14] are quite constant, essentially independent of the liquids used; the average value is $\gamma_{sv} = 34.4 \pm 0.8\,\mathrm{mJ/m^2}$. This reconfirms the soundness of the approach to calculate solid surface tensions from contact angles.

Acknowledgements

This research was supported by the Natural Science and Engineering Research Council of Canada (Grants: No. A8278 and No. EQP173469), Ontario Graduate Scholarships (D.Y.K.) and University of Toronto Open Fellowships (D.Y.K.).

References

[1] Derjaguin, B. J., Muller, V. M. and Toporov, Y. P., *J. Colloid Interface Sci.* **73**, 293 (1980).
[2] Johnson, K. L., Kendall, K. and Roberts, A. D., *Proc. Roy. Soc. (London)* **A324**, 301 (1971).
[3] Muller, V. M., Yushchenko, V. S. and Derjaguin, B. V., *J. Colloid Interface Sci.* **92**, 92 (1983).
[4] Fogden, A. and White, L. R., *J. Colloid Interface Sci.* **138**, 414 (1990).
[5] Pashley, R. M., McGuiggan, P. M., Horn, R. G. and Ninham, B. W., *J. Colloid Interface Sci.* **126**, 569 (1988).
[6] Christenson, H. K., *J. Phys. Chem.* **90**, 4 (1986).
[7] Claesson, P. M., Blom, C . E., Horn, P. C. and Ninham, B. W., *J. Colloid Interface Sci.* **114**, 234 (1986).
[8] Pashley, R. M., McGuiggan, P. M. and Pashley, R. M., *Colloids Surf.* **27**, 277 (1987).
[9] Pashley, R. M., McGuiggan, P. M., Ninham, B. W. and Evans, D. F., *Science* **229**, 1088 (1985).
[10] Zisman, W. A., "Contact Angle, Wettability and Adhesion" in *Advances in Chemistry Series* **43** (American Chemical Society, Washington, D. C., 1964).
[11] Fowkes, F. M., *Ind. Eng. Chem.* **12**, 40 (1964).
[12] Driedger, O., Neumann, A .W. and Sell, P. J., *Kolloid-Z. Z. Polym.* **201**, 52 (1965).
[13] Neumann, A. W., Good, R. J., Hope, C. J. and Sejpal, M., *J. Colloid Interface Sci.* **49**, 291 (1974).
[14] Spelt, J. K. and Li, D., "The Equation of State Approach to Interfacial Tensions" in *Applied Surface Thermodynamics*, Neumann, A. W. and Spelt, J. K., Eds. (Marcel Dekker Inc., New York, 1996), pp. 239–292.
[15] Owens, D. K. and Wendt, R. C., *J. Appl. Polym. Sci.* **13**, 1741 (1969).
[16] van Oss, C. J., Chaudhury, M. K. and Good, R. J., *Chem. Revs.* **88**, 927 (1988).
[17] Good, R. J. and van Oss, C. J., "The Modern Theory of Contact Angles and the Hydrogen Bond Components of Surface Energies" in *Modern Approaches to Wettability: Theory and Applications*, Schrader, M. and Loeb, G., Eds. (Plenum Press, New York, 1992), pp. 1–27.

[18] Bruil, H. G., *Colloid Polym. Sci.* **252**, 32 (1974).
[19] Cheever, G. D., *J. Coat Technol.* **55**, 53 (1983).
[20] Kilau, H. W., *Colloids Surf.* **26**, 217 (1983).
[21] Grundke, D., Bogumil, T., Gietzelt, T., Jacobasch, H.-J., Kwok, D. Y. and Neumann, A. W., *Progr. Colloid Polym. Sci.* **101**, 58 (1996).
[22] Vargha-Butler, E. I., Zubovits, T. K., Absolom, D. R. and Neumann, A. W., *Dispersion Sci. Technol.* **6**(3), 357 (1985).
[23] Vargha-Butler, E. I., Moy, E. and Neumann, A. W., *Colloids Surf.* **24**, 315 (1987).
[24] Vargha-Butler, E. I., Zubovits, T. K., Absolom, D. R. and Neumann, A. W., *Chem. Eng. Commun.* **33**, 255 (1985).
[25] Li, D. and Neumann, A. W., "Wettability and Surface Tension of Particles" in *Applied Surface Thermodynamics*, Neumann, A. W. and Spelt, J. K., Eds. (Marcel Dekker Inc., New York, 1996), pp. 509-556.
[26] Omenyi, S. N. and Neumann, A. W., *J. Appl. Phys.* **47**, 3956 (1976).
[27] Li, D. and Neumann, A. W., "Behavior of Particles at Solidification Fronts" in *Applied Surface Thermodynamics*, Neumann, A. W. and Spelt, J. K., Eds. (Marcel Dekker Inc., New York, 1996), pp. 557-628.
[28] Moy, E. and Neumann, A. W., "Theoretical Approaches for Estimating solid-liquid Interfacial Tensions" in *Applied Surface Thermodynamics*, Neumann, A. W. and Spelt, J. K., Eds. (Marcel Dekker Inc., New York, 1996), pp. 333-378.
[29] Neumann, A. W., *Adv. Colloid Interface Sci.* **4**, 105 (1974).
[30] Marmur, A., *Colloids Surf. A* **116**, 25 (1996).
[31] Li, D. and Neumann, A. W., "Thermodynamic Status of Contact Angles" in *Applied Surface Thermodynamics*, Neumann, A. W. and Spelt, J. K., Eds. (Marcel Dekker Inc., New York, 1996), pp. 109-168.
[32] Sedev, R. V., Petrov, J. G. and Neumann, A. W., *J. Colloid Interface Sci.* **180**, 36 (1996).
[33] Kwok, D. Y., Li, D. and Neumann, A. W., "Capillary Rise at a Vertical Plate as a Contact Angle Technique" in *Applied Surface Thermodynamics*, Neumann, A. W. and Spelt, J. K., Eds. (Marcel Dekker Inc., New York, 1996), pp. 413-440.
[34] Kwok, D. Y., Budziak, C. J. and Neumann, A. W., *J. Colloid Interface Sci.* **173**, 143 (1995).
[35] Kwok, D. Y., Lin, R., Mui, M. and Neumann, A. W., *Colloids Surf. A* **116**, 63 (1996).
[36] Kwok, D. Y., Gietzelt, T., Grundke, K., Jacobasch, H.-J. and Neumann, A. W., *Langmuir* **13**, 2880 (1997).
[37] Kwok, D. Y., Lam, C. N. C., Li, A., Leung, A. and Neumann, A. W., "Low-Rate Dynamic Contact Angles on Non-Inert Poly(propene-*alt*-N-(*n*-alkyl)maleimide) Copolymers by an Automated Axisymmetric Drop Shape Analysis (ADSA-P)", *Langmuir* **14**, 2548 (1998).
[38] Kwok, D. Y., Lam, C. N. C., Li, A., Leung, A., Wu, R., Mok, E. and Neumann, A. W., "Measuring and Interpreting Contact Angles: A Complex Issue", *Colloids Surf. A* (accepted for publication).
[39] del Rio, O. I., Kwok, D. Y., Wu, R., Alvarez, J. M. and Neumann, A. W., "Contact Angle Measurements by Axisymmetric Drop Shape Analysis and an Automated Polynomial Fit Program" *Colloid Surf. A* (accepted for publication).
[40] Kwok, D. Y., Leung, A., Lam, C .N. C., Li, A., Wu, R. and Neumann, A. W., "Low-Rate Dynamic Contact Angles on Poly(methyl methacrylate) and the Determination of Solid Surface Tensions", *J. Colloid Interface Sci.* (accepted for publication).
[41] Kwok, D. Y., Leung, A., Li, A., Lam, C. N. C., Wu, R. and Neumann, A. W., "Low-Rate Dynamic Contact Angles on Poly(*n*-butyl methacrylate) and the Determination of Solid Surface Tensions", *Colloid Polym. Sci.* (accepted for publication).

[42] Kwok, D. Y., Lam, C. N. C., Li, A., Zhu, K., Wu, R. and Neumann, A. W., "Low-Rate Dynamic Contact Angles on Polystyrene and the Determination of Solid Surface Tensions", *Polym. Eng. Sci.* (accepted for publication).
[43] Grundke, K., Weidenhammer, P., Werner, P., Trinowitz, R., Janke, A., Kwok, D. Y., Pöschel, K., Jacobasch, H.-J. and Neumann, A. W. (in preparation).
[44] Oliver, J. F., Huh, C. and Mason, S. G., *J. Colloid Interface Sci.* **59**, 568 (1977).
[45] Oliver, J. F., Huh, C. and Mason, S. G., *Colloids Surf.* **1**, 79 (1980).
[46] Rotenberg, Y., Boruvka, L. and Neumann, A. W., *J. Colloid Interface Sci.* **93**, 169 (1983).
[47] Cheng, P., Li, D., Boruvka, L., Rotenberg, Y. and Neumann, A. W., *Colloids Surf.* **93**, 169 (1983).
[48] Lahooti, S., del Rio, O. I., Cheng, P. and Neumann, A. W., "Axisymmetric Drop Shape Analysis" in *Applied Surface Thermodynamics*, Neumann, A. W. and Spelt, J. K., Eds. (Marcel Dekker Inc., New York, 1996), pp. 441–507.
[49] Duncan, D., Li, D., Gaydos, J. and Neumann, A. W., *J. Colloid Interface Sci.* **169**, 256 (1995).
[50] Gaydos, J. and Neumann, A. W., "Line Tension in Multiphase Equilibrium Systems" in *Applied Surface Thermodynamics*, Neumann, A. W. and Spelt, J. K., Eds. (Marcel Dekker Inc., New York, 1996), pp. 169–238.
[51] Shanahan, M. E. R., *Langmuir* **11**, 1041 (1995).
[52] Li, D. and Neumann, A. W., *J. Colloid Interface Sci.* **148**, 190 (1992).
[53] Li, D., Xie, M. and Neumann, A. W., *Colloid Polym. Sci.* **271**, 573 (1993).
[54] Kwok, D. Y., Li, D. and Neumann, A. W., *Colloids Surf. A* **89**, 181 (1994).
[55] Antonow, G., *J. Chim. Phys.* **5**, 372 (1907).
[56] Berthelot, D., *Compt. Rend.* **126: 1703**, 1857 (1898).
[57] Li, D. and Neumann, A. W., *J. Colloid Interface Sci.* **137**, 304 (1990).
[58] van Giessen, A. E., Bukman, D. J. and Widom, B., *J. Colloid Interface Sci.* **192**, 257 (1997).